MOLECULAR AND CELLULAR BIOLOGY, Feb. 2008, p. 1298–1312 Vol. 28, No. 4
0270-7306/08/$08.00+0 doi:10.1128/MCB.00936-07

Pat1 Contains Distinct Functional Domains That Promote P-Body Assembly and Activation of Decapping▽

Guy R. Pilkington and Roy Parker*

Department of Molecular and Cellular Biology and Howard Hughes Medical Institute, University of Arizona, Tucson, Arizona 85721-0106

Received 25 May 2007/Returned for modification 6 July 2007/Accepted 25 October 2007

The control of mRNA degradation and translation are important aspects of gene regulation. Recent results suggest that translation repression and mRNA decapping can be intertwined and involve the formation of a quiescent mRNP, which can accumulate in cytoplasmic foci referred to as P bodies. The Pat1 protein is a key component of this complex and an important activator of decapping, yet little is known about its function. In this work, we analyze Pat1 in *Saccharomyces cerevisiae* function by deletion and functional analyses. Our results identify two primary functional domains in Pat1: one promoting translation repression and P-body assembly and a second domain promoting mRNA decapping after assembly of the mRNA into a P-body mRNP. In addition, we provide evidence that Pat1 binds RNA and has numerous domain-specific interactions with mRNA decapping factors. These results indicate that Pat1 is an RNA binding protein and a multidomain protein that functions at multiple stages in the process of translation repression and mRNA decapping.

A critical aspect of the regulation of eukaryotic gene expression is the control of mRNA turnover. In eukaryotes, two major pathways for the decay of mRNAs exist, both of which are initiated by deadenylation, with the predominant nuclease being the Ccr4/Pop2/Not1-5 deadenylase complex (31, 35). Following deadenylation, the transcript is susceptible to one of the two pathways of decay. In the 3′-to-5′ decay pathway, the deadenylated mRNA is degraded 3′ to 5′ by a complex of proteins known as the exosome (1). Alternatively, the mRNA is decapped by the decapping enzyme (Dcp1/Dcp2), the mechanism that predominates in *Saccharomyces cerevisiae*, making the mRNA susceptible to the 5′-to-3′ exonuclease Xrn1 (4, 18, 19, 24, 32). Decapping is modulated by a set of proteins including Dhh1, the Lsm1-7 complex, Edc1-3, and Pat1 (7, 16, 22, 44).

Decapping is a critical node in the control of the life of an mRNA. Moreover, the processes of mRNA decapping and translation are mechanistically intertwined and appear to compete with each other, at least in yeast (14). For example, decreasing translation initiation by a variety of means increases the rate of mRNA decapping (28, 33, 39). Conversely, inhibition of translation elongation leads to a significant decrease in the rate of decapping (3). Moreover, coimmunoprecipitation experiments suggested that prior to decapping, an mRNA exits translation and then assembles into a translationally repressed messenger ribonucleoprotein (mRNP) complex (45).

Additional evidence for a discrete population of nontranslating mRNPs has been that nontranslating mRNAs and the decapping machinery accumulate in discrete cytoplasmic foci called P bodies (also referred as GW182 or Dcp bodies) (17, 25, 30, 40). P bodies have now been observed in yeast, insect cells, nematodes, and mammalian cells and contain various proteins involved in mRNA decay, including the decapping enzyme (Dcp1/Dcp2); activators of decapping, Dhh1, Pat1, Lsm1-7, and Edc3; and the exonuclease Xrn1 (2, 20, 34). Moreover, P bodies have been suggested to be functionally involved in mRNA decapping (17, 40), nonsense-mediated decay (41, 46), mRNA storage (6, 9), general translation repression (15, 23), microRNA-mediated repression (26, 29, 36), and, possibly, viral packaging (5). In these cases, the analysis of P bodies, translation repression, and decapping suggests that the process of translation repression and mRNA decapping involves an initial step wherein the mRNA ceases translation and assembles an mRNP capable of decapping and accumulation in P bodies. This initial step would then be followed by a subsequent decapping reaction, although the relationship between translation repression, P-body mRNP assembly, and actual catalysis of decapping remains unclear.

An important protein in the process of mRNA decapping and translation repression is Pat1. Yeast strains lacking Pat1 show the strongest defects in decapping of any mutant besides defects in the decapping enzyme Dcp1/Dcp2 (7, 8, 44). In addition, efficient translation repression during glucose deprivation and P-body assembly requires Pat1 (15, 23, 42). Moreover, the overexpression of Pat1 leads to a global repression of translation and accumulation of mRNAs in P bodies (15). Pat1 is also a conserved protein and is found in P bodies in *Saccharomyces cerevisiae*, *Drosophila melanogaster*, and mammalian cells as well (15, 20, 38, 40). Despite this central role in mRNA decapping, P-body assembly, and translation repression, the properties of the Pat1 and its functional interactions are unknown.

In this work, we analyze Pat1 function in *Saccharomyces cerevisiae* by deletion and functional analyses. Our results indicate that Pat1 contains two important functional domains: one that promotes translation repression and P-body assembly and another one that promotes mRNA decapping in a manner enhanced by the assembly of the transcript into a P-body

* Corresponding author. Mailing address: Department of Molecular and Cellular Biology and Howard Hughes Medical Institute, University of Arizona, 1007 E. Lowell St., Tucson, AZ 85721-0206. Phone: (520) 621-9347. Fax: (520) 621-4524. E-mail: rrparker@u.arizona.edu.
▽ Published ahead of print on 17 December 2007.

TABLE 1. Yeast strains used in this study

Strain	Genotype	Reference or source
yRP840	*MAT***a** *leu2-3,112 trp1 ura3-52 his4-39 cup1*Δ*::LEU2/PGK1pG/MFA2pG*	21
yRP1372	*MAT***a** *leu2-3,112 trp1 ura3-52 his4-39 cup1*Δ*::LEU2/PGK1pG/MFA2pG pat1*Δ*::LEU2*	44
yRP2228	*MAT*α *leu2-3,112 trp1 ura3-52 his4-39 cup1*Δ*::LEU2/PGK1pG/MFA2pG pat1*Δ*::LEU2* LSM1-GFP (NEO)	42
yRP2386	*MAT*α *leu2-3,112 lys2-201 ura3-52 cup1*Δ*::LEU2/PGK1pG/MFA2pG* Kan^r-GAL-GST-PAT1	This study
yRP2387	*MAT*α *leu2-3,112 lys2-201 ura3-52 cup1*Δ*::LEU2/PGK1pG/MFA2pG* Kan^r-GAL-GST-PAT1:Δ1-10	This study
yRP2388	*MAT*α *leu2-3,112 lys2-201 ura3-52 cup1*Δ*::LEU2/PGK1pG/MFA2pG* Kan^r-GAL-GST-PAT1:Δ1-131	This study
yRP2389	*MAT*α *leu2-3,112 lys2-201 ura3-52 cup1*Δ*::LEU2/PGK1pG/MFA2pG* Kan^r-GAL-GST-PAT1:Δ1-254	This study
yRP2390	*MAT*α *leu2-3,112 lys2-201 ura3-52 cup1*Δ*::LEU2/PGK1pG/MFA2pG* Kan^r-GAL-GST-PAT1:Δ1-422	This study
yRP2391	*MAT*α *leu2-3,112 lys2-201 ura3-52 cup1*Δ*::LEU2/PGK1pG/MFA2pG* Kan^r-GAL-GST-PAT1:Δ1-697	This study
yRP2392	*MAT*α *leu2-3,112 lys2-201 ura3-52 cup1*Δ*::LEU2/PGK1pG/MFA2pG* Kan^r-GAL-GST-PAT1:Δ1-797	This study
yRP2093	*MAT*α *trp1-901 leu2-3,112 ura3-52 his3-200 gal4*Δ *gal80*Δ *LYS2::GAL1-HIS3 GAL2-ADE2 met2::GAL7-lacz* [pOBD-2]	Decker et al., unpublished
yRP2364	*MAT***a** *trp1-901 leu2-3,112 ura3-52 his3-200 gal4*Δ *gal80*Δ *LYS2::GAL1-HIS3 GAL2-ADE2 met2::GAL7-lacz* [pOAD]	Decker et al., unpublished
yRP2368	*MAT***a** *trp1-901 leu2-3,112 ura3-52 his3-200 gal4*Δ *gal80*Δ *LYS2::GAL1-HIS3 GAL2-ADE2 met2::GAL7-lacz* [pOADEDC3]	Decker et al., unpublished
yRP2183	*MAT***a** *leu2-3,112 trp1 ura3-52 his4-39 lys2-201 cup1*Δ*::LEU2/PGK1pG/MFA2pG pat1*Δ*::LEU2* DCP2-GFP (NEO)	42

mRNP. In addition, we provide evidence that Pat1 binds RNA and has numerous domain-specific interactions with mRNA decapping factors. These results indicate that Pat1 is an RNA binding protein and a multidomain protein that functions at multiple stages in the process of translation repression and mRNA decapping.

MATERIALS AND METHODS

Yeast strains and plasmids. The genotypes of strains used in this study are listed in Table 1. Strains were grown on either standard yeast extract-peptone medium or synthetic complete (SC) medium supplemented with the appropriate amino acids and 2% glucose as a carbon source. Strains were grown at 30°C unless otherwise stated.

All plasmids used in this study are listed in Table 2. Deletion constructs of Pat1 were made by inserting a blunt-cutting restriction endonuclease into the respective sites by means of QuikChange mutagenesis according to the manufacturer's instructions (Stratagene, CA).

Western blot. In order to detect the levels of protein expression of the Pat1 deletion constructs, we made Flag epitope-tagged versions of all the deletion constructs by means of QuikChange mutagenesis according to the manufacturer's instructions (Stratagene). These constructs were then transformed into *pat1*Δ strains, grown at 30°C to an optical density at 600 nm (OD_{600}) of 0.6, lysed in a 5 M urea–2% sodium dodecyl sulfate (SDS) solution, and then loaded onto an SDS–10% polyacrylamide gel. Electrophoresed samples were transferred onto a Protran nitrocellulose membrane (Whatman, NJ) and then probed with anti-Flag antibody (Sigma).

RNA analysis. For mRNA decapping analysis of the yeast reporter mRNA MFA2pG, cells were grown to an OD_{600} of 0.3 to 0.4 in SC medium supplemented with the appropriate amino acid and 2% galactose at 30°C. Cells were harvested and total RNA was extracted as described previously by Caponigro et al. (12). RNA was analyzed by running 20 μg of total RNA on 6% urea-polyacrylamide gels. Northern analyses were performed using a radiolabeled oligonucleotide, oRP140, which is directed against the MFA2pG reporter mRNA (13). Quantitation of blots was performed using a Molecular Dynamics (Sunnyvale, CA) PhosphorImager. Loading corrections were done using oRP100, an oligonucleotide directed against 7S RNA, a stable RNA polymerase III transcript (11).

After repeating the assay with newly transformed strains on three separate occasions, we performed statistical analysis on the resulting quantitation. A Mann-Whitney nonparametric test was performed on the results to determine if a statistically significant difference was observed between the deletion constructs. This ranking-based test allowed us to group those constructs that showed differences from the *pat1*Δ strain with a P value of less than 0.02.

Microscopy. High-optical-density cultures were grown to an OD_{600} of 1.0 in the appropriate medium. Cells were washed in SC medium supplemented with the appropriate amino acids without glucose, resuspended in the same medium, incubated in a flask in a shaking water bath for 10 min, and then collected by centrifugation. In the case of the cells at the mid-log phase of growth, they were grown to an OD_{600} of 0.3 to 0.5 in the appropriate medium with glucose. An aliquot of cells was then resuspended in the same medium for observation by use of the fluorescent microscope. Cells were observed on a Leica DM-RXA fluorescent microscope equipped with a mercury xenon light source. Images were captured by use of a Retiga EX (Q Imaging) digital camera and manipulated using Metamorph 6.0 software.

For analysis of P bodies following galactose induction, cells were grown in minimal medium supplemented with 2% sucrose to an OD_{600} of 0.3 to 0.4. At this point, the cells were washed in minimal medium, split in to two equal subcultures: one subculture was resuspended in minimal medium plus 2% sucrose, while the other subculture was resuspended in minimal medium plus 2% galactose. Following 120 min of induction, aliquots of cells were concentrated on a tabletop centrifuge, resuspended in their respective media, and observed on a Leica DM-RXA fluorescent microscope.

Yeast two-hybrid analysis. The two-hybrid fusion plasmids were constructed by PCR amplification of the open reading frame (ORF) of the indicated genes or the Pat1 ORF deleted for certain domains and inserted into pOAD or pOBD-2 by homologous recombination in yeast strains PJ694a and PJ694α as described previously (10, 27). PJ694a strains containing pOAD alone or pOAD containing full-length Lsm1, Edc3, or Dcp1 were mated with PJ694α strains containing pOBD-2 alone or pOBD-2 with full-length Pat1 or Pat1 deletions. Interactions were measured by β-galactosidase plate assays as well as 3-amino-1,2,4-triazol dilution series assays.

Translational repression analysis. In vivo [^{35}S]methionine labeling was performed by growing cells in minimal medium containing 2% sucrose, harvesting 12 ml of cells at an OD_{600} of 0.3, and then resuspending cells in 20 ml minimal medium containing 2% sucrose or 2% galactose plus 0.25% sucrose for 120 min to induce Pat1 overexpression. Cells were then labeled by adding 120 μl cold

TABLE 2. Plasmids used in this study

Primer	Description	Vector	Insert	Source
pRP1469	Pat1:Δ10-763	Ycplac33 (pRP1305)	Pat1 with residues 10–763 deleted	This study
pRP1470	Pat1:Δ131-763	Ycplac33 (pRP1305)	Pat1 with residues 131–763 deleted	This study
pRP1471	Pat1:Δ254-763	Ycplac33 (pRP1305)	Pat1 with residues 254–763 deleted	This study
pRP1472	Pat1:Δ422-763	Ycplac33 (pRP1305)	Pat1 with residues 422–763 deleted	This study
pRP1473	Pat1:Δ697-763	Ycplac33 (pRP1305)	Pat1 with residues 697–763 deleted	This study
pRP1474	Pat1:Δ10-697	Ycplac33 (pRP1305)	Pat1 with residues between 10 and 697 deleted	This study
pRP1475	Pat1:Δ10-422	Ycplac33 (pRP1305)	Pat1 with residues between 10 and 422 deleted	This study
pRP1476	Pat1:Δ10-254	Ycplac33 (pRP1305)	Pat1 with residues between 10 and 254 deleted	This study
pRP1477	Pat1:Δ10-131	Ycplac33 (pRP1305)	Pat1 with residues between 10 and 131 deleted	This study
pRP1478	Pat1:Full	Ycplac33 (pRP1305)	Full-length Pat1	This study
pRP1479	Pat1:Δ254-422	Ycplac33 (pRP1305)	Pat1 with residues between 254 and 422 deleted	This study
pRP1480	Pat1:Δ422-697	Ycplac33 (pRP1305)	Pat1 with residues between 422 and 697 deleted	This study
pRP1481	Pat1:Δ10-763 + Flag	Ycplac33 (pRP1305)	Pat1 with residues 10–763 deleted + Flag	This study
pRP1482	Pat1:Δ131-763 + Flag	Ycplac33 (pRP1305)	Pat1 with residues 131–763 deleted + Flag	This study
pRP1483	Pat1:Δ254-763 +Flag	Ycplac33 (pRP1305)	Pat1 with residues 254–763 deleted + Flag	This study
pRP1484	Pat1:Δ422-763 + Flag	Ycplac33 (pRP1305)	Pat1 with residues 422–763 deleted + Flag	This study
pRP1485	Pat1:Δ697-763 + Flag	Ycplac33 (pRP1305)	Pat1 with residues 697–763 deleted + Flag	This study
pRP1486	Pat1:Δ10-697 + Flag	Ycplac33 (pRP1305)	Pat1 with residues between 10 and 697 deleted + Flag	This study
pRP1487	Pat1:Δ10-422 + Flag	Ycplac33 (pRP1305)	Pat1 with residues between 10 and 422 deleted + Flag	This study
pRP1488	Pat1:Δ10-254 + Flag	Ycplac33 (pRP1305)	Pat1 with residues between 10 and 254 deleted + Flag	This study
pRP1489	Pat1:Δ10-131 + Flag	Ycplac33 (pRP1305)	Pat1 with residues between 10 and 131 deleted + Flag	This study
pRP1490	Pat1:Full + Flag	Ycplac33 (pRP1305)	Full-length Pat1 + Flag	This study
pRP1491	Pat1:Δ254-422 + Flag	Ycplac33 (pRP1305)	Pat1 with residues between 254 and 422 deleted + Flag	This study
pRP1492	Pat1:Δ422-697 + Flag	Ycplac33 (pRP1305)	Pat1 with residues between 422 and 697 deleted + Flag	This study
pRP1493	Pat1:Δ10-763 + GFP	Ycplac33 (pRP1305)	Pat1 with residues 10–763 deleted + GFP	This study
pRP1494	Pat1:Δ131-763 + GFP	Ycplac33 (pRP1305)	Pat1 with residues 131–763 deleted + GFP	This study
pRP1495	Pat1:Δ254-763 + GFP	Ycplac33 (pRP1305)	Pat1 with residues 254–763 deleted + GFP	This study
pRP1496	Pat1:Δ422-763 + GFP	Ycplac33 (pRP1305)	Pat1 with residues 422–763 deleted + GFP	This study
pRP1497	Pat1:Δ697-763 + GFP	Ycplac33 (pRP1305)	Pat1 with residues 697–763 deleted + GFP	This study
pRP1498	Pat1:Δ10-697 + GFP	Ycplac33 (pRP1305)	Pat1 with residues between 10 and 697 deleted + GFP	This study
pRP1499	Pat1:Δ10-422 + GFP	Ycplac33 (pRP1305)	Pat1 with residues between 10 and 422 deleted + GFP	This study
pRP1500	Pat1:Δ10-254 + GFP	Ycplac33 (pRP1305)	Pat1 with residues between 10 and 254 deleted + GFP	This study
pRP1501	Pat1:Δ10-131 + GFP	Ycplac33 (pRP1305)	Pat1 with residues between 10 and 131 deleted + GFP	This study
pRP1502	Pat1:Full + GFP	Ycplac33 (pRP1305)	Full-length Pat1 + GFP	This study
pRP1503	Pat1:Δ254-422 + GFP	Ycplac33 (pRP1305)	Pat1 with residues between 254 and 422 deleted + GFP	This study
pRP1504	Pat1:Δ422-697 + GFP	Ycplac33 (pRP1305)	Pat1 with residues between 422 and 697 deleted + GFP	This study
pRP1505	Pat1:Δ10-763	poBD-II (pRP1289)	Pat1 with residues 10–763 deleted	This study
pRP1506	Pat1:Δ131-763	poBD-II (pRP1289)	Pat1 with residues 131–763 deleted	This study
pRP1507	Pat1:Δ254-763	poBD-II (pRP1289)	Pat1 with residues 254–763 deleted	This study
pRP1508	Pat1:Δ422-763	poBD-II (pRP1289)	Pat1 with residues 422–763 deleted	This study
pRP1509	Pat1:Δ697-763	poBD-II (pRP1289)	Pat1 with residues 697–763 deleted	This study
pRP1510	Pat1:Δ10-697	poBD-II (pRP1289)	Pat1 with residues between 10 and 697 deleted	This study
pRP1511	Pat1:Δ 10-422	poBD-II (pRP1289)	Pat1 with residues between 10 and 422 deleted	This study
pRP1512	Pat1:Δ10-254	poBD-II (pRP1289)	Pat1 with residues between 10 and 254 deleted	This study
pRP1513	Pat1:Δ10-131	poBD-II (pRP1289)	Pat1 with residues between 10 and 131 deleted	This study
pRP1514	Pat1:Full	poBD-II (pRP1289)	Full-length Pat1	This study
pRP1515	Pat1:Δ254-422	poBD-II (pRP1289)	Pat1 with residues between 254 and 422 deleted	This study
pRP1516	Pat1:Δ422-697	poBD-II (pRP1289)	Pat1 with residues between 422 and 697 deleted	This study
pRP1517	Pat1:Full	poAD (pRP1290)	Full-length Pat1	This study
pRP1518	Lsm1	poAD (pRP1290)	Lsm1 ORF	This study
pRP1519	Dcp1	poAD (pRP1290)	Dcp1 ORF	This study
pRP1520	Pat1:Full	pTNT	pTNT in vitro expression vector + Pat1:Full	This study
pRP1521	Pat1:residues 10-254	pTNT	pTNT in vitro expression vector + Pat1:residues 10-254	This study
pRP1522	Pat1:residues 254-422	pTNT	pTNT in vitro expression vector + Pat1:residues 254-422	This study
pRP1523	Pat1:residues 422-763	pTNT	pTNT in vitro expression vector + Pat1:residues 422-763	This study

methionine (10 μg/ml) and 3 μl [^{35}S]methionine (Amersham). At the determined time points, 1-ml aliquots were added to 1 ml 20% trichloroacetic acid. Samples were heated at 95°C for 20 min, collected on Whatman glass microfiber paper, washed with 10% trichloroacetic acid and 95% ethyl alcohol, and placed in scintillation fluid. This solution was then quantified on a scintillation counter.

In vitro translation and RNA binding assays. In vitro translation of 1 μg of Pat1-containing plasmid was performed with the TNT quick-coupled reticulocyte lysate system (Promega) according to the manufacturer's instructions. In vitro translation was performed in the presence of 20 μCi of in vitro translation-grade [^{35}S]methionine (Amersham). The binding of in vitro-translated, [^{35}S]methionine-labeled Pat1 and Pat1 deletion constructs to RNA homopolymers was performed according to the following protocol. Poly(U)-Sepharose and protein G-Sepharose (Promega) were prepared according to the manufacturer's recommendations and resuspended at a concentration corresponding to 100 μg (dry weight) per ml in binding buffer (10 mM Tris [pH 7.4], 2.5 mM $MgCl_2$, 100 mM KCl, and 0.5% Triton X-100). Twenty-five microliters of poly(U)-Sepharose or protein G-Sepharose was mixed with 10 μl of full-length Pat1 in vitro-translated product, 10 μl of the product at residues 10 to 254, 100 μl of the product at residues 254 to 422, and 100 μl of the product at residues 422 to 763. This solution was mixed in a total of 300 μl in the presence of 200 U of RNasin and 0.5 μg/ml of yeast tRNA as a nonspecific competitor and incubated at 4°C for 45 min. In competition experiments, poly(U) or poly(C) (Amersham) was added to

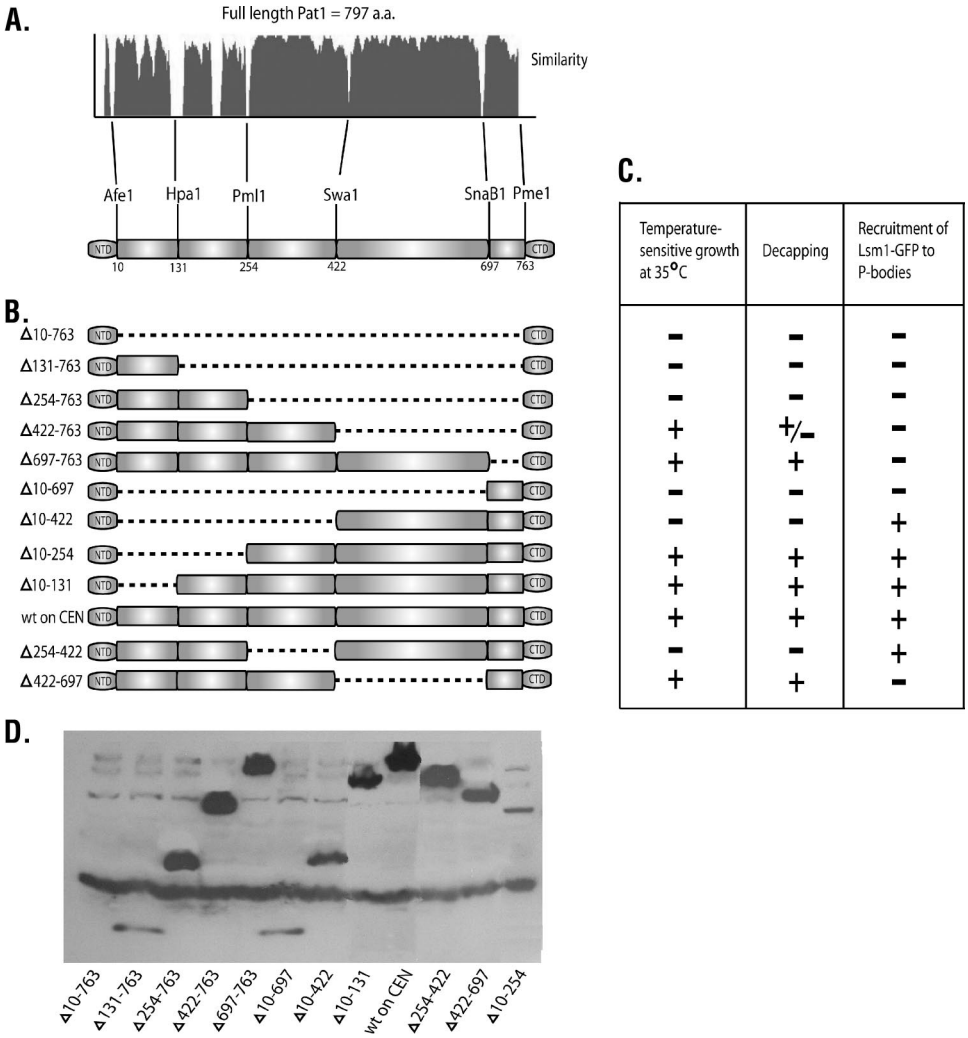

FIG. 1. Deletion constructs of Pat1. (A) Regions of homology from a fungal alignment. Pat1 fungal homologs from *S. cerevisiae*, *S. paradoxus*, *S. mikatae*, *S. bayanus*, *S. castellii*, and *S. kudriavzevii* were downloaded from the *Saccharomyces* Genome Database and imported into Vector NTI (Invitrogen, CA). We then aligned the sequences using the AlignX module of Vector NTI and determined the regions of similarity from within the alignment module. CTD, C-terminal domain; NTD, N-terminal domain. (B) Format of the deletion constructs used to determine functional domains of Pat1 showing placement of the blunt-cutting restriction endonucleases. (C) Observed phenotypes of the respective deletion constructs. (D) Western blot showing expression levels of the Pat1 deletion constructs. wt, wild type.

the binding reaction mixtures at the concentrations indicated in the figures. Following the binding reaction, the Sepharose beads were washed four times in binding buffer, resuspended in sample buffer, boiled for 2 min, and loaded onto an SDS–12% polyacrylamide gel. Following electrophoresis, the gels were exposed to PhosphorImager screens, and quantitation of blots was performed using a Molecular Dynamics (Sunnyvale, CA) PhosphorImager.

RESULTS

General strategy. To understand the role of yeast Pat1 in mRNA decapping and translation repression, we undertook a deletion analysis to identify functional regions and to identify specific regions of Pat1 that interact with other decapping factors and/or RNA. To target these deletions to functional domains of Pat1, we positioned the end points of the deletions at the ends of regions of higher amino acid conservation based upon an alignment of all the Pat1 homologues in the collection of sequenced fungus genomes. When Pat1 proteins from *Saccharomyces* species are aligned together, regions of high homology and regions of low homology became evident, suggesting discrete organizational domains (Fig. 1A). This domain structure is conserved in Pat1 orthologs from more complex eukaryotes as well, although the specific domains are not as highly conserved (data not shown). Using this comparison, we created a series of in-frame deletions (see Materials and Methods) by removing one or more conserved regions (Fig. 1B). Each deletion construction was expressed under its native promoter from a low-copy-number centromere (CEN) plasmid in a *pat1*Δ strain and tested for its effect on Pat1 function in a variety of assays. In addition, to maintain the proper context of translation initiation and termination, 10 amino acids from the N terminus and 34 amino acids from the C terminus were included in each construct. We also observed a single amino acid change in the yRP840 genome sequence compared to the

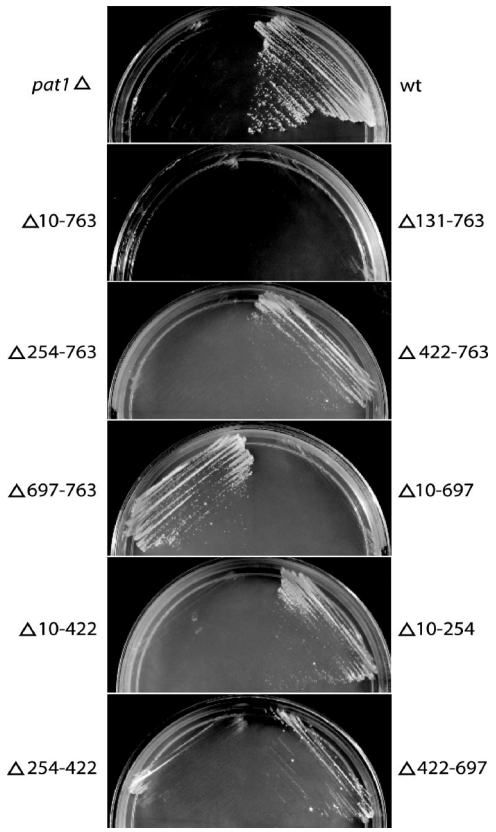

FIG. 2. Residues 254 to 422 of Pat1 are required for growth at 35°C in a *pat1*Δ strain. Shown is growth of *pat1*Δ yeast cells at 35°C transformed with plasmids containing empty vector (*pat1*Δ), wild-type Pat1 (wt), or the deletion constructs. Yeast strains were grown on minimal medium plates supplemented with 2% dextrose and placed at 35°C for 3 days.

Saccharomyces Genome Database sequence (V688D); however, this appears to have no functional consequences, since our PAT1-containing plasmids are functionally no different from wild-type PAT1 (data not shown).

Residues 254 to 422 define a domain required for growth at high temperatures. It is known that *pat1*Δ strains are temperature sensitive and are unable to grow at 35°C. Analysis of the various Pat1 deletions revealed that any construct lacking residues 254 to 422 (Δ254-422) was unable to grow at 35°C (Fig. 1C and 2). In contrast, Pat1 variants lacking residues 10 to 254 or 422 to 763 were still able to grow at 35°C, although strains expressing Pat1 lacking residues 422 to 763 were slightly growth impaired at high temperatures. These results define the domain between residues 254 and 422 as being the critical part of Pat1 for growth at high temperatures.

Most Pat1 deletion variants are expressed as stable proteins. One potential reason for a *pat1*Δ variant showing a defect in function would be due to the deletion protein being unstable and being present only at reduced concentrations compared to wild-type Pat1. In order to examine this possibility, we tagged the different Pat1 deletion variants with a Flag epitope at their N termini, which did not affect Pat1 protein function, and examined their levels by Western blotting. Four relevant observations were observed in these experiments. First, the Δ254-763, Δ422-763, Δ697-763, Δ10-422, Δ10-131, Δ254-422, and Δ422-697 variants were all expressed at levels similar to those of the full-length protein (Fig. 1D). Therefore, any phenotype arising from these deletions cannot be due to reduced levels of Pat1 (see below). Second, we observed that the Δ10-254 variant was consistently expressed at lower levels than the full-length protein (Fig. 1D and data not shown). Surprisingly, despite this reduced level of expression, this deletion had no effect on cell growth and has only a small effect on decapping efficiency (see below). These observations suggest that reductions in the level of Pat1 can be tolerated without strong phenotypes. Third, we observed that the Pat1 variants with large deletions (Δ10-763, Δ131-763, and Δ10-697) were expressed at reduced levels (Fig. 1D), although this does not impact the conclusions drawn from variants with smaller deletions (see below). Finally, as previously noted (47), we observed that Pat1 and its deletion variants ran anomalously for their predicted molecular weights on SDS gels.

The domain between residues 254 and 422 is required for Pat1 to stimulate decapping, and two other domains enhance the ability of Pat1 to activate decapping. A second phenotype of *pat1*Δ strains is a defect in the rate of mRNA decapping (7, 8, 21, 44). Thus, we examined how different deletions in Pat1 affected mRNA decapping in yeast. To this end, we analyzed the unstable MFA2pG reporter RNA, which contains a poly(G) tract within the MFA2 3′ untranslated region (18). The poly(G) tract is an effective block of 5′-to-3′ exonucleolytic decay resulting in the formation of a decay intermediate referred to as the poly(G) fragment. With this reporter mRNA, *pat1*Δ strains show two differences from wild-type strains, indicating their defect in mRNA decapping. First, because deadenylation precedes decapping, *pat1*Δ strains accumulate a population of deadenylated mRNAs (Fig. 3A, lane 1, compared to the wild type on CEN, lane 11). Second, due to the decreased rate of decapping, the levels of the poly(G) fragment, whose abundance can be related to the decapping rate of the mRNA, are decreased (11). Thus, to examine how different domains of Pat1 affected mRNA decapping, we examined which constructs led to the loss of accumulation of deadenylated full-length mRNAs and restored the production of the poly(G) fragment.

Examination of the deletions for their effect on decapping revealed the following points. First, residues 254 to 422 were required for Pat1 to promote decapping, and any construct lacking this region, including a precise deletion of residues 254 to 422, was similar to *pat1*Δ in decapping efficiency (Fig. 3A, compare lane 12 to the wild type on CEN, lane 11). Second, residues 10 to 254 also had a small effect on decapping (Δ10-254) (Fig. 3A), although this effect could be due to the reduced levels of this particular deletion protein, or this region might be able to enhance decapping in some manner (Fig. 1D). Third, residues 422 to 763 affect the efficiency of mRNA decapping since any deletion of this region, including the precise deletion of residues 422 to 763 (lane 5), gives a partial defect in mRNA decapping without affecting protein levels. However, it should be noted that the domain at residues 422 to 763 appears to act through the region at residues 254 to 422 since strains containing the region at residues 422 and 763 without the region at residues 254 to 422 still show an absolute block in decapping (Fig. 3A, lane 12, and B). Taken together, these results indi-

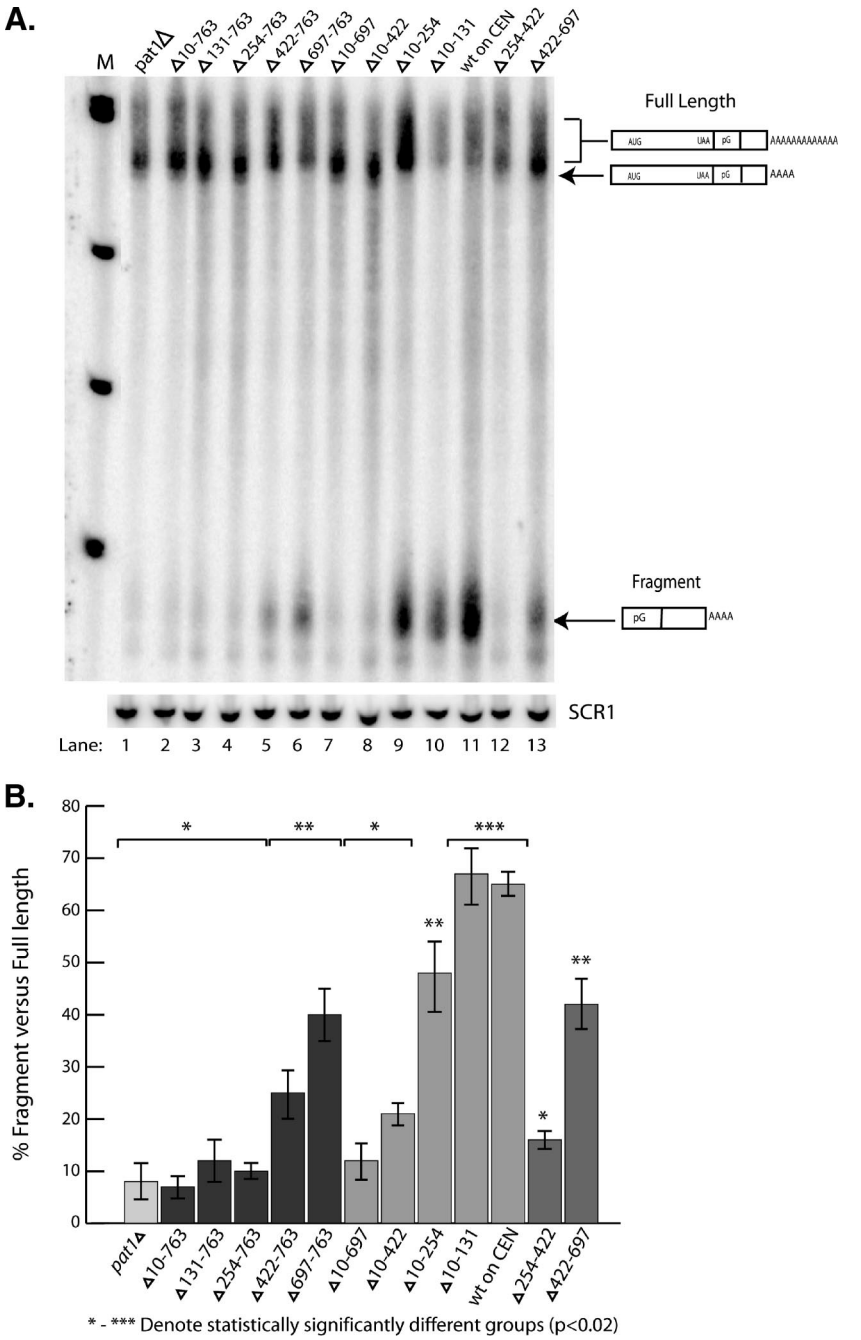

FIG. 3. Residues 254 to 422 of Pat1 are required for the restoration of decapping in a *pat1*Δ strain. (A) Shown is the steady-state decay analysis of the unstable MFA2 reporter mRNA in a *pat1*Δ strain. Each lane represents the strain containing empty vector (*pat1*Δ), wild-type PAT1 on a CEN vector (wt on CEN), or deletion constructs. SCR1 RNA is shown below each panel as a loading control. The diagram indicates the relative positions of the full-length mRNA and the poly(G) decay intermediate. M indicates the molecular size marker. (B) Graph depicting the relative percentages of the poly(G) decay fragment versus full-length mRNA for *pat1*Δ, the wild type on the CEN plasmid, and each respective deletion construct-containing *pat1*Δ strain. Error bars indicate ranges of values obtained. Asterisks indicate groupings that showed statistically significant differences from each other assessed by a Mann-Whitney nonparametric test and with a *P* value of less than 0.02.

cate that two regions of Pat1 can directly affect decapping, with residues 254 to 422 being absolutely required for Pat1 to stimulate decapping and residues 422 to 763 affecting the efficiency with which residues 254 to 422 can promote decapping.

The region at residues 422 to 763 is responsible for the role of Pat1 in translation repression and P-body assembly. Pat1 has been shown to accumulate in P bodies (40), to inhibit translation and promote P-body formation when overexpressed (15), and to be required for the recruitment of Lsm1 to P bodies (42). To identify the regions of Pat1 that affected these three events, we examined how the different deletion constructs affected Pat1 accumulation in P bodies, Lsm1 re-

cruitment to P bodies, and translation repression and P-body formation when overexpressed.

The region at residues 422 to 763 is required for Lsm1-GFP to accumulate in P bodies. Previous work has shown that the ability of Lsm1-green fluorescent protein (GFP) to accumulate in P bodies is dependent on the presence of Pat1 (34). To determine what region(s) of Pat1 was required for Lsm1 recruitment to P bodies, we examined the presence of an Lsm1-GFP fusion protein in cells at high cell densities where P bodies are large and easily visualized (43). A formal caveat of these experiments is that we are examining a GFP-tagged version of Lsm1. However, since Lsm1-GFP was previously shown to require Pat1 function for localization to P bodies (41), and untagged Lsm1 is found in mammalian P bodies (25), this is a valid approach to studying Lsm1-GFP localization. As shown in Fig. 4, the distinct foci of Lsm1-GFP seen in a wild-type PAT1 background were no longer evident in the *pat1*Δ strain. Moreover, any Pat1 construct that lacked the region at residues 422 to 763 was deficient in recruiting Lsm1 to P bodies (constructs Δ10-763 through Δ697-763) (Fig. 4), including a precise deletion of this region (Δ422-763). Note that both the region between residues 422 and 697 and the region between residues 697 and 763 are required for the recruitment of Lsm1 to P bodies by Pat1. In contrast, the regions at residues 10 to 254 and 254 to 422 are dispensable for the recruitment of Lsm1 to P bodies (constructs Δ10-254 and Δ254-422). This defines the region at residues 422 to 763 as being required for the recruitment of Lsm1, and presumably the entire Lsm1-7 complex, to P bodies.

In order to test if residues 422 to 763 of Pat1 along with the N- and C-terminal amino acids present in all constructs were sufficient to recruit Lsm1-GFP to P bodies, we expressed a Pat1 variant that contained residues 422 to 763. As shown in Fig. 4, the Δ10-422 construct was effectively able to form foci of Lsm1-GFP, indicating that residues 422 to 763 are both necessary and sufficient (along with the N- and C-terminal amino acids) for the recruitment of Lsm1-GFP to P bodies.

The region at residues 422 to 763 is required for Pat1-GFP to accumulate in P bodies. The data described above suggest that the region at residues 422 to 763 of Pat1 is required for the recruitment of Lsm1 to P bodies. The simplest explanation for this observation is that this region of Pat1 is required for Pat1 itself to accumulate in P bodies. To test this possibility, we fused a C-terminal GFP to Pat1 deletion variants lacking either residues 10 to 254 (a region that appeared to have no function yet), residues 254 to 422 (which were required for Pat1 to promote decapping), or residues 422 to 763 (which were required for the recruitment of Lsm1 to P bodies). We observed that residues 10 to 254 and 254 to 422 were not required for Pat1 to accumulate in P bodies (Fig. 5). In contrast, we observed that the region between residues 422 and 763 was required for Pat1 to localize to P bodies. This defines residues 422 to 763 as being required to target Pat1 to P bodies. Moreover, this suggests that residues 422 to 763 are required for Pat1 to recruit Lsm1, at least in part, by first localizing Pat1 to P bodies.

Inhibition of growth and translational repression by Pat1 overexpression requires residues 422 to 697. Previous work has shown that the overexpression of Pat1 from a galactose promoter inhibited cell growth, reduced translation, and increased the number of P bodies (15). To determine what portion of Pat1 was required for this growth inhibition and P-body accumulation, we used the galactose-inducible (GAL) promoter to drive the expression of various Pat1 deletions and determined which region was required for the inhibition of cell growth and P-body accumulation (Fig. 6A). For these experiments, we replaced the PAT1 promoter in the chromosome with a GAL promoter since we observe stronger inhibition of growth from Pat1 overexpression when the construct is in the chromosome (data not shown). In addition, the construct contains a glutathione *S*-transferase (GST) tag to allow us to examine the levels of the overexpressed protein, which were all similar (data not shown). Due to integration into the chromosome, it should be noted that these deletion variants lack the N-terminal 10 amino acids present in the Pat1 variants expressed from plasmids, although the similar phenotypes of the full-length protein and construct 2 in Fig. 6 suggest that this region is not functionally important.

Similar to previously reported results (15), we observed that the overexpression of a full-length GST-Pat1 fusion protein inhibited cell growth, increased P-body formation, and reduced translation, as judged by the incorporation of [^{35}S]methionine in vivo (Fig. 6B, C, D, and E). Moreover, we observed that the overexpression of Pat1 variants lacking the first 10 amino acids (construct 2), amino acids 1 to 131 (construct 3), amino acids 1 to 254 (construct 4), and amino acids 1 to 422 (construct 5) were still able to inhibit growth, increase the accumulation of P bodies, and reduce translation (Fig. 6B, C, D, and E). In contrast, the overexpression of Pat1 variants lacking amino acids 1 to 697 (construct 6) or amino acids 1 to 797 (construct 7, with essentially no Pat1) failed to decrease growth, enhance P-body formation, or inhibit translation (Fig. 6B, C, D, and E). These results demonstrate that the region at residues 422 to 797 of Pat1 is sufficient to inhibit growth, promote P-body formation, and inhibit translation when overexpressed.

Pat1 function in P-body assembly is upstream of decapping. The data described above suggest a sequential model for Pat1 function. In the first step, the region of Pat1 between amino acids 422 and 763 first inhibits translation, increases the assembly of mRNPs that can accumulate in P bodies, and correspondingly has some effect on decapping efficiency. In this model, a second step in decapping would be promoted by the region between amino acids 254 and 422, which is enhanced by the translation repression/assembly function of residues 422 to 763. A prediction of this model is that different lesions in Pat1 should affect the accumulation of P bodies in different manners in a mid-log-phase culture, where yeast P bodies are typically small (40). Specifically, we predict that *pat1*Δ variants lacking amino acids 422 to 763 should lead to reduced P bodies compared to wild-type cells due to a defect in accumulation, whereas *pat1*Δ variants lacking just the region at residues 254 to 422 should show greatly increased levels of P bodies. Moreover, a larger deletion removing both regions would be expected have reduced levels of P bodies. To test these predictions, we examined the accumulation of Dcp2-GFP in various *pat1*Δ strains during mid-log-phase growth, where P bodies are small and increases in P-body size and number are easy to observe (41).

Consistent with the predictions described above, we observed that strains expressing Δ422-763 showed a reduction in

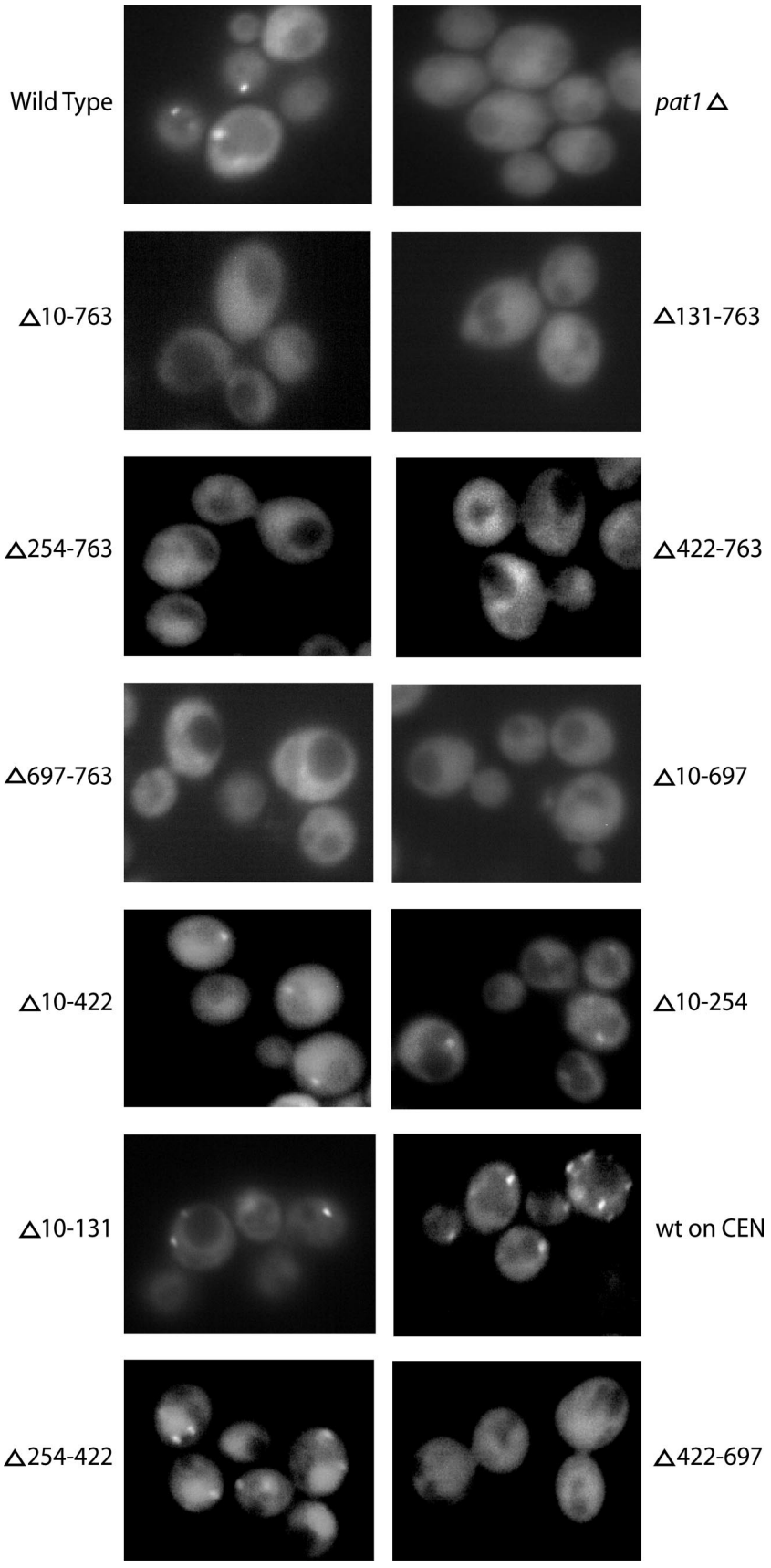

FIG. 4. Residues 422 to 763 of Pat1 are required for Lsm1-GFP to accumulate in P bodies. Using Lsm1-GFP as a marker for P bodies, we observed P bodies in either a wild-type (wt), *pat1*Δ, or deletion construct-containing *pat1*Δ strain.

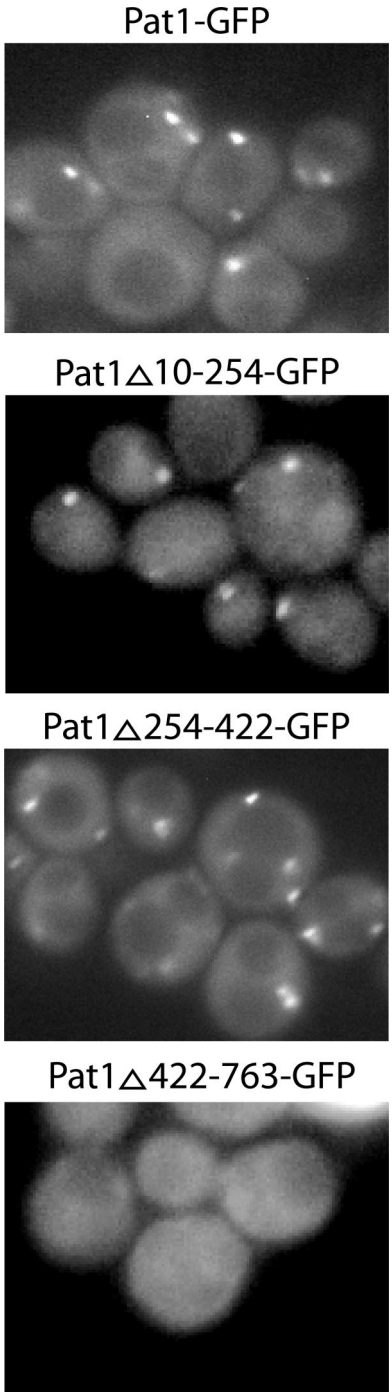

FIG. 5. Residues 422 to 763 of Pat1 are required for Pat1-GFP to accumulate in P bodies. *pat1*Δ strains were transformed with plasmids containing deletion constructs of Pat1 tagged with a C-terminal GFP. P bodies were observed only in constructs that contained residues 422 to 763.

the number of P-body-containing cells compared to the strains expressing the full-length Pat1, supporting the claim that the region at residues 422 to 763 affects P-body assembly (Fig. 7A and B). In contrast, strains expressing Δ254-422 showed an increase in the number and size of P bodies compared to the strains expressing full-length Pat1 (Fig. 7A and B). This is consistent with the region at residues 254 to 422 being required only for a late step in decapping after the formation of an mRNP that can accumulate in P bodies. Moreover, strains expressing Pat1 variants lacking both the region at residues 254 to 422 and the region at residues 422 to 763 (Δ10-763 and Δ254-763) showed levels of P bodies similar to that of the Δ422-763 construct alone. This indicates that the accumulation of P bodies seen in the Δ254-422 strain is dependent on the ability of Pat1 to promote P-body assembly.

Specific domains of Pat1 mediate interactions with Lsm1, Dcp1, and Edc3. The above-described results have identified two important regions of Pat1. One is the region between residues 254 and 422, which is required for activating decapping. A second important region is between residues 422 and 763, which is required for the assembly of Pat1 and Lsm1 into P bodies and for growth inhibition and translational repression when overexpressed. This suggests a model of Pat1 function that involves an initial function in the assembly of a translationally repressed mRNP followed by a function in triggering actual decapping. In order to understand how these two regions could be executing these functions, we examined the nature of physical interactions between these two domains and other proteins within P bodies as well as the ability of Pat1 and its subdomains to bind RNA.

Two-hybrid interactions reveal Pat1 interactions with Dcp1, Lsm1, and Edc3. To identify candidates for proteins that directly interact with Pat1, we screened for strong interactions between Pat1 and other components of P bodies by two-hybrid analysis. We observed that Pat1 showed strong two-hybrid interactions with Lsm1, Dcp1, and Edc3 (Fig. 8A). Following the initial identification of proteins that interact with Pat1, we used the Pat1 deletions to map the specific regions of Pat1 in which the interactions occur. It was determined that the Lsm1-Pat1 two-hybrid interaction requires amino acids 254 to 422 of Pat1, while the Pat1-Dcp1 and Pat1-Edc3 two-hybrid interactions required amino acids 422 to 797 (Fig. 8A).

The interaction of Pat1 with Edc3 was interesting since Edc3 contains an N-terminal Lsm domain, a central FDF domain of unknown function containing the amino acid motif FDF, and a C-terminal Yjef-N domain. These different domains play specific scaffolding roles in Edc3 in both the assembly of a Dcp1-Dcp2-Dhh1-Edc3 complex and the aggregation of individual mRNPs into larger P bodies (C. J. Decker, D. Texeira, and R. Parker, unpublished data). In order to determine which region of Edc3 interacted with Pat1, we tested the individual Edc3 domains for their abilities to interact with Pat1. We observed that Pat1 interacted only with the Lsm domain of Edc3, thus defining this domain as the Pat1 interaction site on Edc3 (Fig. 8B).

Pat1 is an RNA binding protein. The role of Pat1 in translation repression and mRNA decapping suggested that Pat1 might be an RNA binding protein. Moreover, the *Xenopus* ortholog of Pat1, P100, is capable of binding to DNA, although RNA binding was not tested in those experiments (37). In order to directly test if yeast Pat1 binds to RNA, we used RNA homopolymers bound to Sepharose beads as a means of assessing Pat1 binding to RNA. Pat1 was translated in the presence of [^{35}S]methionine in an in vitro transcription and translation reaction. The lysate from this reaction was then incubated in the presence of poly(U)-bound Sepharose beads.

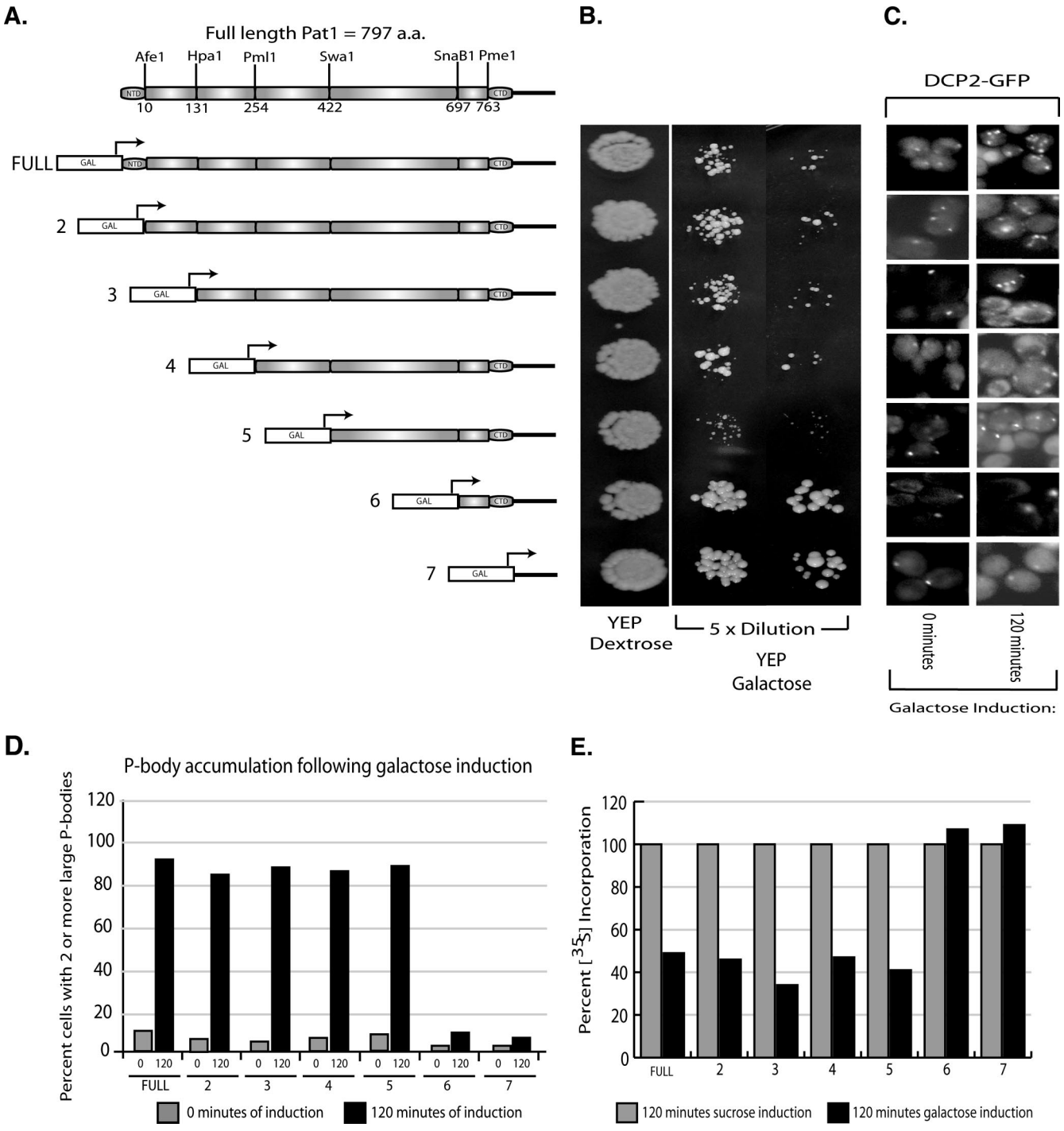

FIG. 6. Residues 422 to 697 of Pat1 are required for the overexpression growth defect, P-body increase, and translational repression caused by Pat1. (A) Cartoon illustrating the construction of the chromosomally integrated galactose overexpression cassettes of Pat1 deletions. The KanMX6 GAL upstream activating sequence GST cassette was integrated upstream of full-length PAT1 as well as each respective PAT1 deletion, allowing the galactose-driven overexpression of each respective construct. CTD, C-terminal domain; NTD, N-terminal domain. (B) Growth of yeast cells of each respective construct when plated on galactose medium. YEP, yeast extract-peptone. (C) P-body accumulation in cells following overexpression of the respective constructs. Times after the addition of galactose are indicated. P bodies were visualized using Dcp2-GFP. (D) Histogram showing the percentage of P-body-containing cells with two or more large, visible P bodies per cell both pre- and postinduction with galactose for each respective PAT1 deletion. (E) Histogram showing incorporation of [^{35}S]methionine in cells overexpressing Pat1 deletions 10 min after the addition of label. The values for incorporation following sucrose induction were set as 100% for each deletion strain, and the values for galactose induction are represented as a percentage of the sucrose values.

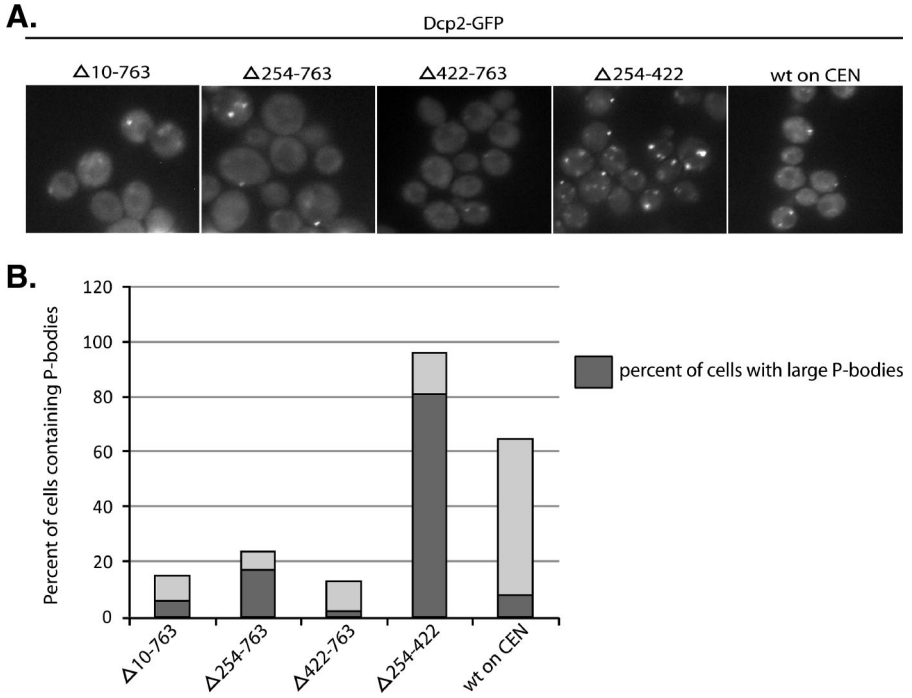

FIG. 7. Residues 422 to 763 of Pat1 are required for Dcp2-GFP to accumulate in P bodies at mid-log phase. (A) Using Dcp2-GFP as a marker for P bodies, we observed P bodies in a mid-log-phase growing *pat1*Δ strain containing the indicated deletion constructs on CEN plasmids. (B) Histogram indicating the percentage of cells for each construct that contained visible P bodies and the proportion of those P bodies that were larger than typical P bodies. wt, wild type.

As shown in Fig. 9, full-length Pat1 efficiently bound to poly(U) homopolymers in the presence of yeast tRNA as a nonspecific competitor (lane 2). This binding was successfully outcompeted in the presence of specific poly(U) competitor (Fig. 9, lanes 3 and 4) but not in the presence of poly(C) (lane 5). This binding was also specific to the poly(U) homopolymer, since no binding occurred when lysate was added to non-homopolymer-containing Sepharose, protein G-Sepharose (Fig. 9, lane 6). This observation indicates that Pat1 can bind RNA and shows a preference for poly(U) substrates.

To determine which regions of Pat1 were responsible for RNA binding, we examined the abilities of different regions of Pat1 to bind RNA. Thus, we expressed three regions of Pat1 in vitro: residues 10 to 254, for which we can assign no function to date; residues 254 to 422, which are required for decapping; and residues 422 to 763, which function in translation repression and P-body assembly. We observed that residues 10 to 254 did not bind poly(U)-Sepharose (Fig. 9, lane 8), while both the region at residues 254 to 422 and the region at residues 422 to 763 did effectively bind to poly(U) homopolymers (Fig. 9, lanes 11 and 14, respectively). Similarly to full-length Pat1, this binding was specific since it was outcompeted by the presence of free poly(U) (Fig. 9, lanes 12 and 15, respectively). This provides evidence that Pat1 has two independent RNA binding domains localized to residues 254 to 422 and 422 to 763.

DISCUSSION

Understanding Pat1 function. In this work, we examine the function and interactions of Pat1. Pat1 is of significant interest since *pat1*Δ strains show a strong defect in mRNA decapping (7, 8, 21, 44) and have defects in translational repression during glucose deprivation (15, 23). Our results indicate that Pat1 plays two separable roles in the process of translation repression and mRNA decapping. In addition, we provide evidence that Pat1 binds RNA and has numerous interactions with mRNA decapping factors. As discussed in detail below, our results suggest a preliminary and initial model of Pat1 function wherein Pat1 first interacts with translating mRNAs through one or more domain to contribute to translation repression and the assembly of a P-body mRNP, followed by a second domain of Pat1 functioning to increase the actual rate of decapping following the formation of the P-body mRNP (Fig. 10).

The domain at residues 422 to 763 of Pat1 promotes translation repression and P-body assembly. Several observations indicate that Pat1 residues between 422 and 763 function to promote translation repression and P-body assembly. First, this domain is required for Pat1 to promote translation repression and the accumulation of P bodies when overexpressed (Fig. 6). Second, this domain is required for Pat1 to be able to accumulate in P bodies (Fig. 5). Third, and consistent with it being required for Pat1 recruitment into P bodies, this domain is required for the recruitment of Lsm1, and presumably the entire Lsm1-7 complex, into P bodies (Fig. 4 and 7). Taken together, we suggest that the domain at residues 422 to 763 of Pat1 functions to repress translation in a yet-to-be-defined manner and then promotes the subsequent assembly of the mRNA decapping complex including Dcp1, Dcp2, Edc3, and the Lsm1-7 complex on the mRNA, which can then aggregate

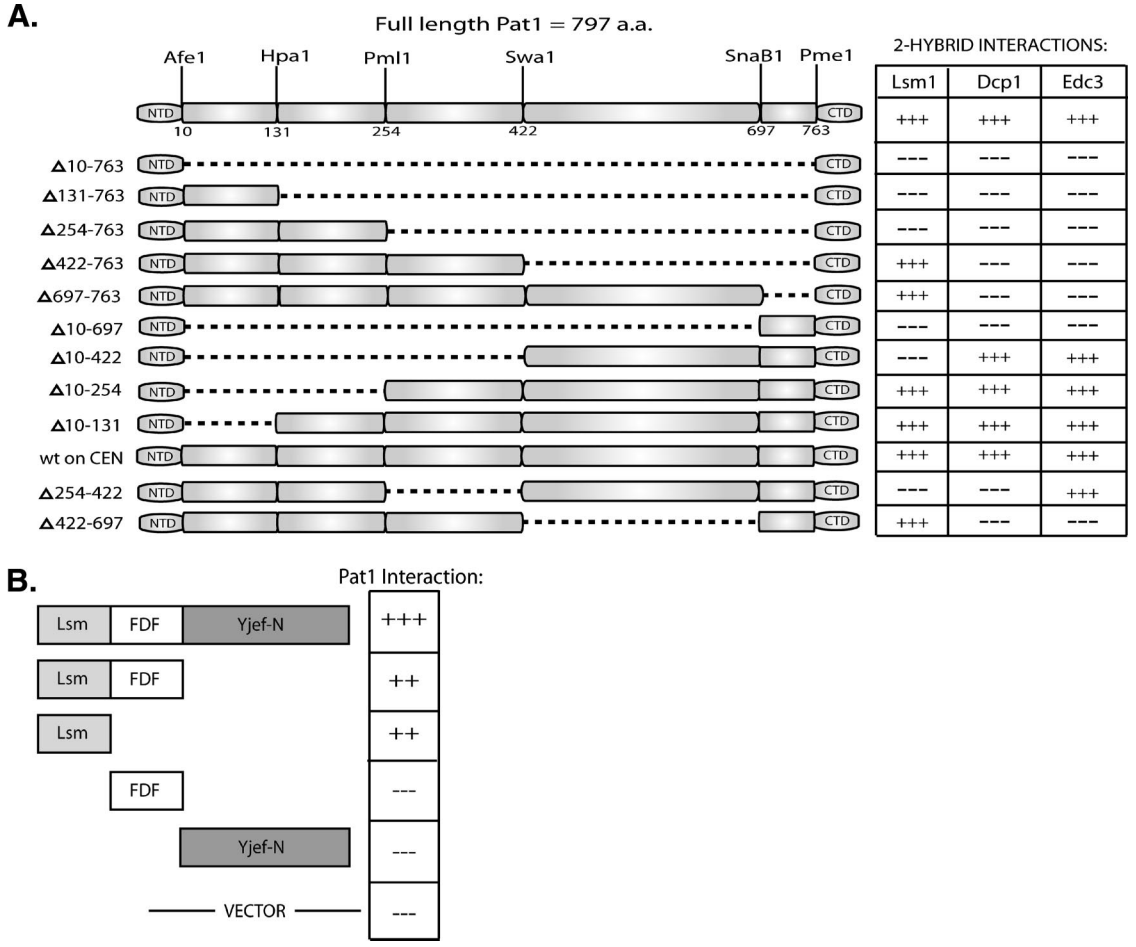

FIG. 8. Lsm1, Dcp1, and Edc3 interact with different domains of Pat1, and Pat1 interacts with the Lsm domain of Edc3. (A) Using a two-hybrid analysis, we determined that Lsm1, Dcp1, and Edc3 all interact with full-length Pat1. By repeating the two-hybrid analysis with the deletion constructs of Pat1, we showed the specific regions of Pat1 with which the proteins interact. +++ indicates a strong interaction with Pat1, while – – – indicates no interaction with Pat1. a.a., amino acids; NTD, N-terminal domain; CTD, C-terminal domain. (B) Using a two-hybrid analysis, we determined the interaction of Pat1 with domains of Edc3. Pat1 specifically interacts with the Lsm domain of Edc3. +++ indicates a strong interaction with Pat1, while – – – indicates no interaction with Pat1. FDF, FDF amino acid motif.

in P bodies. This role of Pat1 in the recruitment of Dcp1/Dcp2 and the Lsm1-7 complex is consistent with previous work demonstrating an interaction between the Lsm1-7 complex and Pat1 (7, 44, 45) and our observations of interactions of the domain at residues 422 to 763 of Pat1 with Dcp1 and Edc3 (Fig. 8).

One unresolved issue is why residues 422 to 763 are sufficient to recruit Lsm1, and presumably the entire Lsm1-7 complex, to P

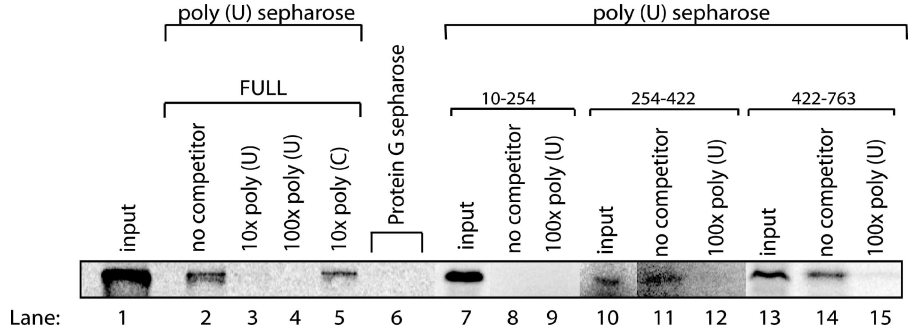

FIG. 9. Pat1 binds to RNA homopolymers. Binding of in vitro-translated [^{35}S]methionine-labeled Pat1 and Pat1 domains to poly(U)-Sepharose was done in the presence of yeast tRNA at 0.5 μg/ml as a nonspecific competitor. Binding reactions were carried out in the presence of specific competitors at 10- and 100-fold excesses. No binding to the protein G-Sepharose occurred. Lanes marked input show 10% of the volume of the in vitro-translated products used for the binding reaction of full-length Pat1, 10% of the volume for residues 10 to 254, 5% of the volume for residues 254 to 422, and 5% of the volume for residues 422 to 763.

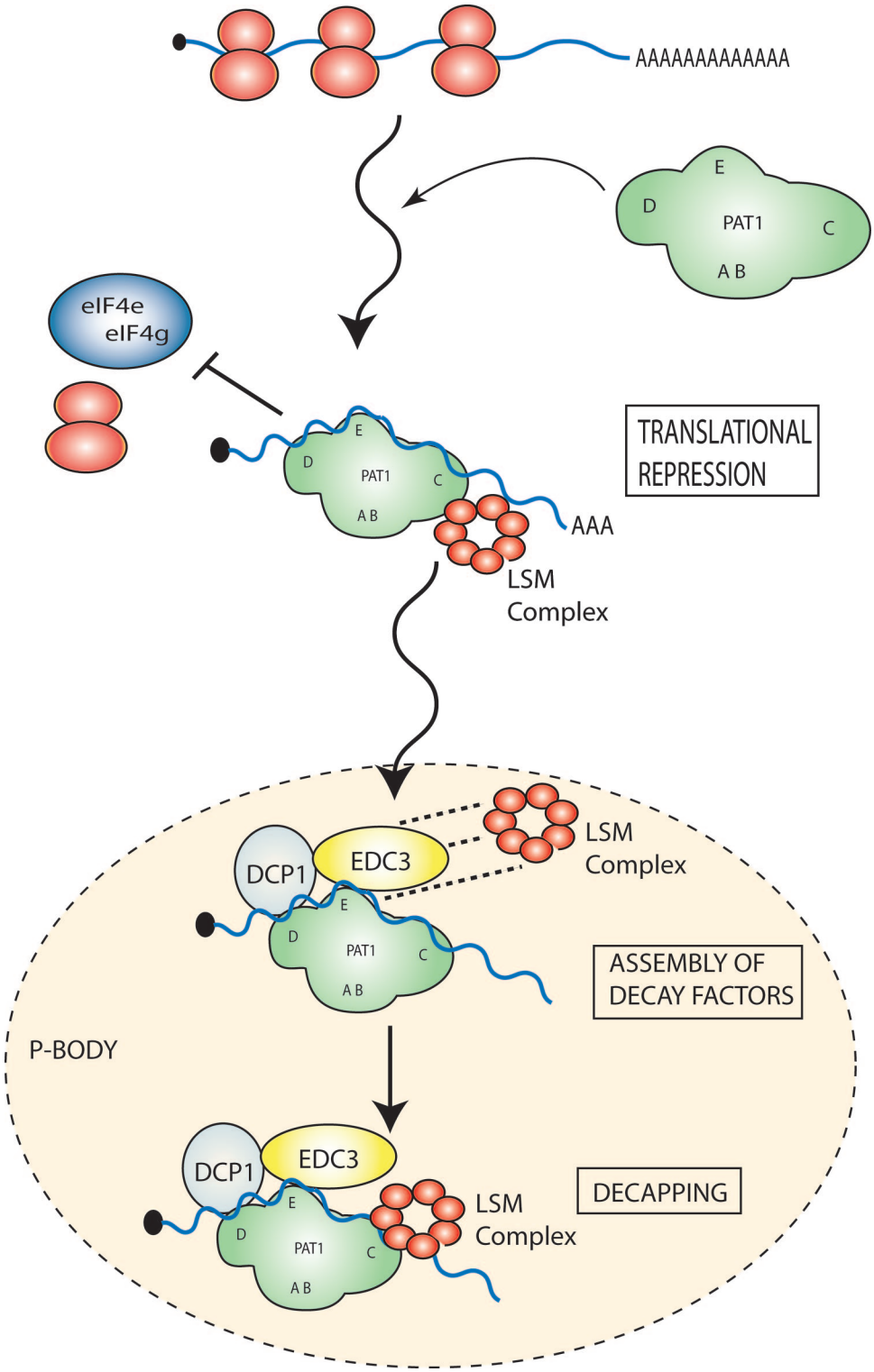

FIG. 10. Model for Pat1 function. LSM complex, Lsm1-7 protein complex.

bodies when only residues 254 to 422 showed interactions with Lsm1. We consider two possible explanations. First, it could be that there are additional interactions between the Lsm1-7 complex and Pat1 that we have not detected in the two-hybrid assay. Second, it could be that Pat1 binding to the P-body complex induces conformational changes in other proteins that then promote Lsm1-7 interactions with those components. Future experiments should be able to distinguish these possibilities.

The domain at residues 254 to 422 of Pat1 promotes mRNA decapping after P-body assembly. Several observations identify

Pat1 residues 254 to 422 as functioning to promote mRNA decapping after translation repression and the assembly of a P-body mRNP. The critical observation is that any Pat1 deletion construct lacking the domain at residues 254 to 422 is as defective in mRNA decapping as a *pat1*Δ strain (Fig. 3). In contrast, Pat1 deletion variants lacking the region at residues 254 to 422 are still able to assemble into P bodies (Fig. 5), recruit Lsm1-GFP and Dcp2-GFP to P bodies, and inhibit growth when overexpressed (Fig. 4, 6, and 7). Moreover, strains expressing Pat1 lacking the region at residues 254 to 422 accumulate large P bodies during mid-log-phase growth, consistent with a block to decapping (Fig. 7) Taken together, these observations suggest that the domain at residues 254 to 422 functions after the assembly of a translationally repressed mRNP that can accumulate in P bodies. Consistent with that view, the domain at residues 254 to 422 binds to Lsm1-7, which is known to affect decapping at a late stage after the assembly of an mRNP that can accumulate in P bodies (42).

An unresolved issue is the molecular event that the domain at residues 254 to 422 facilitates to promote decapping. One possibility is that additional interactions between the mRNA and/or additional decapping factors with this region of Pat1 stabilize the P-body mRNP and that this enhanced stability provides prolonged times for decapping. However, this model seems unlikely since we observed that the deletion of this region increases P-body formation (Fig. 7) and promotes even stronger translation repression when overexpressed (Fig. 6), which is consistent with the Δ254-422 construct leading to a block to decapping after the assembly of the P-body mRNP. Given this finding, a more likely possibility is that the domain at residues 254 to 422 functions to promote a conformational change in the P-body mRNP that activates the decapping enzyme (either by directly facilitating the formation of a more active conformation or by removing some inhibitory interactions).

Our results suggest that the function of the domain at residues 422 to 763 influences the ability of the domain at residues 254 to 422 to promote decapping. The key observation is that Pat1 variants lacking any part of the domain at residues 422 to 763 show a reduction in decapping efficiency (Fig. 3). Moreover, the residual decapping seen in the Δ422-763 variants is dependent on the region at residues 254 to 422 since variants lacking both residues 254 to 422 and 422 to 763 show no function of Pat1 in decapping (Fig. 3). These results are consistent with Pat1 functioning to first promote translation repression and the assembly of a P-body mRNP committed to decapping within which the region at residues 254 to 422 of Pat1 could function to enhance the actual rate of catalysis for decapping.

Pat1 is an RNA binding protein with two independent RNA binding domains. In this work, we also provide evidence that Pat1 is an RNA binding protein. The critical observation is that in vitro-synthesized Pat1 binds to poly(U)-Sepharose (Fig. 9). Moreover, this binding can be competed by poly(U) but not poly(C), thus suggesting that Pat1 prefers to bind poly(U)-rich RNAs. The ability of Pat1 to bind RNA is consistent with its coimmunoprecipitation with mRNA (45). In addition, it seems likely that this property will be conserved since the *Xenopus* ortholog of Pat1, P100, is capable of binding to DNA, although RNA was not tested in those experiments (37). Finally, because domains at both residues 254 to 422 and 422 to 763 of Pat1 are sufficient by themselves to bind RNA, Pat1 has two regions that can independently bind RNA. Interestingly, the two domains of Pat1 that bind RNA show no resemblance to known RNA binding domains, suggesting that these regions may represent novel RNA binding structures. An important area of future work will be to identify the regions of RNA binding with Pat1 in more detail and determine their preferred binding sequences and functional significances.

ACKNOWLEDGMENTS

We thank the members of the Parker laboratory, especially Carolyn Decker, Ross Buchan, Denise Muhlrad, and Anne Webb, for valuable input, technical support, and useful discussions. We thank Maya Pilkington for her assistance and expertise with the statistical analysis. We also thank J. Cadbury for vital reagents as well as the Department of Molecular and Cellular Biology for the use of their equipment.

An NIH grant (R37 GM45443) and funds from the Howard Hughes Medical Institute supported this work.

REFERENCES

1. **Anderson, J. S., and R. P. Parker.** 1998. The 3′ to 5′ degradation of yeast mRNAs is a general mechanism for mRNA turnover that requires the SKI2 DEVH box protein and 3′ to 5′ exonucleases of the exosome complex. EMBO J. **17:**1497–1506.
2. **Anderson, P., and N. Kedersha.** 2006. RNA granules. J. Cell Biol. **172:**803–808.
3. **Beelman, C. A., and R. Parker.** 1994. Differential effects of translational inhibition in cis and in trans on the decay of the unstable yeast MFA2 mRNA. J. Biol. Chem. **269:**9687–9692.
4. **Beelman, C. A., A. Stevens, G. Caponigro, T. E. LaGrandeur, L. Hatfield, D. M. Fortner, and R. Parker.** 1996. An essential component of the decapping enzyme required for normal rates of mRNA turnover. Nature **382:**642–646.
5. **Beliakova-Bethell, N., C. Beckham, T. H. Giddings, Jr., M. Winey, R. Parker, and S. Sandmeyer.** 2006. Virus-like particles of the Ty3 retrotransposon assemble in association with P-body components. RNA **12:**94–101.
6. **Bhattacharyya, S. N., R. Habermacher, U. Martine, E. I. Closs, and W. Filipowicz.** 2006. Relief of microRNA-mediated translational repression in human cells subjected to stress. Cell **125:**1111–1124.
7. **Bonnerot, C., R. Boeck, and B. Lapeyre.** 2000. The two proteins Pat1 (Mrt1p) and Spb8p interact in vivo, are required for mRNA decay, and are functionally linked to Pab1p. Mol. Cell. Biol. **20:**5939–5946.
8. **Bouveret, E., G. Rigaut, A. Shevchenko, M. Wilm, and B. Seraphin.** 2000. A Sm-like protein complex that participates in mRNA degradation. EMBO J. **19:**1661–1671.
9. **Brengues, M., D. Teixeira, and R. Parker.** 2005. Movement of eukaryotic mRNAs between polysomes and cytoplasmic processing bodies. Science **310:**486–489.
10. **Cagney, G., P. Uetz, and S. Fields.** 2000. High-throughput screening for protein-protein interactions using two-hybrid assay. Methods Enzymol. **328:**3–14.
11. **Cao, D., and R. Parker.** 2001. Computational modeling of eukaryotic mRNA turnover. RNA **7:**1192–1212.
12. **Caponigro, G., D. Muhlrad, and R. Parker.** 1993. A small segment of the *MATα1* transcript promotes mRNA decay in *Saccharomyces cerevisiae*: a stimulatory role for rare codons. Mol. Cell. Biol. **13:**5141–5148.
13. **Caponigro, G., and R. Parker.** 1995. Multiple functions for the poly(A)-binding protein in mRNA decapping and deadenylation in yeast. Genes Dev. **9:**2421–2432.
14. **Coller, J., and R. Parker.** 2004. Eukaryotic mRNA decapping. Annu. Rev. Biochem. **73:**861–890.
15. **Coller, J., and R. Parker.** 2005. General translational repression by activators of mRNA decapping. Cell **122:**875–886.
16. **Coller, J. M., M. Tucker, U. Sheth, M. A. Valencia-Sanchez, and R. Parker.** 2001. The DEAD box helicase, Dhh1p, functions in mRNA decapping and interacts with both the decapping and deadenylase complexes. RNA **7:**1717–1727.
17. **Cougot, N., S. Babajko, and B. Seraphin.** 2004. Cytoplasmic foci are sites of mRNA decay in human cells. J. Cell Biol. **165:**31–40.
18. **Decker, C. J., and R. Parker.** 1993. A turnover pathway for both stable and unstable mRNAs in yeast: evidence for a requirement for deadenylation. Genes Dev. **7:**1632–1643.
19. **Dunckley, T., and R. Parker.** 1999. The DCP2 protein is required for mRNA decapping in *Saccharomyces cerevisiae* and contains a functional MutT motif. EMBO J. **18:**5411–5422.

20. **Eulalio, A., I. Behm-Ansmant, and E. Izaurralde.** 2007. P bodies: at the crossroads of post-transcriptional pathways. Nat. Rev. Mol. Cell Biol. **8:**9–22.
21. **Hatfield, L., C. A. Beelman, A. Stevens, and R. Parker.** 1996. Mutations in *trans*-acting factors affecting mRNA decapping in *Saccharomyces cerevisiae*. Mol. Cell. Biol. **16:**5830–5838.
22. **He, W., and R. Parker.** 2000. Functions of Lsm proteins in mRNA degradation and splicing. Curr. Opin. Cell Biol. **12:**346–350.
23. **Holmes, L. E., S. G. Campbell, S. K. De Long, A. B. Sachs, and M. P. Ashe.** 2004. Loss of translational control in yeast compromised for the major mRNA decay pathway. Mol. Cell. Biol. **24:**2998–3010.
24. **Hsu, C. L., and A. Stevens.** 1993. Yeast cells lacking 5′→3′ exoribonuclease 1 contain mRNA species that are poly(A) deficient and partially lack the 5′ cap structure. Mol. Cell. Biol. **13:**4826–4835.
25. **Ingelfinger, D., D. J. Arndt-Jovin, R. Luhrmann, and T. Achsel.** 2002. The human LSm1-7 proteins colocalize with the mRNA-degrading enzymes Dcp1/2 and Xrnl in distinct cytoplasmic foci. RNA **8:**1489–1501.
26. **Jakymiw, A., S. Lian, T. Eystathioy, S. Li, M. Satoh, J. C. Hamel, M. J. Fritzler, and E. K. Chan.** 2005. Disruption of GW bodies impairs mammalian RNA interference. Nat. Cell Biol. **7:**1267–1274.
27. **James, P., J. Halladay, and E. A. Craig.** 1996. Genomic libraries and a host strain designed for highly efficient two-hybrid selection in yeast. Genetics **144:**1425–1436.
28. **LaGrandeur, T., and R. Parker.** 1999. The cis acting sequences responsible for the differential decay of the unstable MFA2 and stable PGK1 transcripts in yeast include the context of the translational start codon. RNA **5:**420–433.
29. **Liu, J., M. A. Valencia-Sanchez, G. J. Hannon, and R. Parker.** 2005. MicroRNA-dependent localization of targeted mRNAs to mammalian P-bodies. Nat. Cell Biol. **7:**719–723.
30. **Lykke-Andersen, J.** 2002. Identification of a human decapping complex associated with hUpf proteins in nonsense-mediated decay. Mol. Cell. Biol. **22:**8114–8121.
31. **Meyer, S., C. Temme, and E. Wahle.** 2004. Messenger RNA turnover in eukaryotes: pathways and enzymes. Crit. Rev. Biochem. Mol. Biol. **39:**197–216.
32. **Muhlrad, D., C. J. Decker, and R. Parker.** 1994. Deadenylation of the unstable mRNA encoded by the yeast MFA2 gene leads to decapping followed by 5′→3′ digestion of the transcript. Genes Dev. **8:**855–866.
33. **Muhlrad, D., and R. Parker.** 1999. Recognition of yeast mRNAs as "nonsense containing" leads to both inhibition of mRNA translation and mRNA degradation: implications for the control of mRNA decapping. Mol. Biol. Cell **10:**3971–3978.
34. **Parker, R., and U. Sheth.** 2007. P bodies and the control of mRNA translation and degradation. Mol. Cell **25:**635–646.
35. **Parker, R., and H. Song.** 2004. The enzymes and control of eukaryotic mRNA turnover. Nat. Struct. Mol. Biol. **11:**121–127.
36. **Pillai, R. S., S. N. Bhattacharyya, C. G. Artus, T. Zoller, N. Cougot, E. Basyuk, E. Bertrand, and W. Filipowicz.** 2005. Inhibition of translational initiation by Let-7 MicroRNA in human cells. Science **309:**1573–1576.
37. **Rother, R. P., M. B. Frank, and P. S. Thomas.** 1992. Purification, primary structure, bacterial expression and subcellular distribution of an oocyte-specific protein in Xenopus. Eur. J. Biochem. **206:**673–683.
38. **Scheller, N., P. Resa-Infante, S. de la Luna, R. P. Galao, M. Albrecht, L. Kaestner, P. Lipp, T. Lengauer, A. Meyerhans, and J. Diez.** 6 September 2007, posting date. Identification of PatL1, a human homolog to yeast P body component Pat1. Biochim. Biophys. Acta. doi:10.1016/j.bbamcr.2007.08.009.
39. **Schwartz, D. C., and R. Parker.** 1999. Mutations in translation initiation factors lead to increased rates of deadenylation and decapping of mRNAs in *Saccharomyces cerevisiae*. Mol. Cell. Biol. **19:**5247–5256.
40. **Sheth, U., and R. Parker.** 2003. Decapping and decay of messenger RNA occur in cytoplasmic processing bodies. Science **300:**805–808.
41. **Sheth, U., and R. Parker.** 2006. Targeting of aberrant mRNAs to cytoplasmic processing bodies. Cell **125:**1095–1109.
42. **Teixeira, D., and R. Parker.** 2007. Analysis of P-body assembly in *Saccharomyces cerevisiae*. Mol. Biol. Cell **18:**2274–2287.
43. **Teixeira, D., U. Sheth, M. A. Valencia-Sanchez, M. Brengues, and R. Parker.** 2005. Processing bodies require RNA for assembly and contain nontranslating mRNAs. RNA **11:**371–382.
44. **Tharun, S., W. He, A. E. Mayes, P. Lennertz, J. D. Beggs, and R. Parker.** 2000. Yeast Sm-like proteins function in mRNA decapping and decay. Nature **404:**515–518.
45. **Tharun, S., and R. Parker.** 2001. Targeting an mRNA for decapping: displacement of translation factors and association of the Lsm1-7p complex on deadenylated yeast mRNAs. Mol. Cell **8:**1075–1083.
46. **Unterholzner, L., and E. Izaurralde.** 2004. SMG7 acts as a molecular link between mRNA surveillance and mRNA decay. Mol. Cell **16:**587–596.
47. **Wyers, F., M. Minet, M. E. Dufour, L. T. A. Vo, and F. Lacroute.** 2000. Deletion of the *PAT1* gene affects translation initiation and suppresses a *PAB1* gene deletion in yeast. Mol. Cell. Biol. **20:**3538–3549.